WILEY | Hindawi

Research Article

Pasteurella multocida Toxin Aggravates Ligatured-Induced Periodontal Bone Loss and Inflammation via NOD-Like Receptor Protein 3 Inflammasome

Yineng Han [1,2,3] **Pengfei Gao** [4,5] **Qiaolin Yang** [1,2,3] **Yiping Huang** [1,2,3] **Lingfei Jia** [2,3,6] **Yunfei Zheng** [1,2,3] **and Weiran Li** [1,2,3]

[1]*Department of Orthodontics, Peking University School and Hospital of Stomatology, Beijing 100081, China*
[2]*National Center of Stomatology; National Clinical Research Center for Oral Diseases; National Engineering Laboratory for Digital and Material Technology of Stomatology, Beijing 100081, China*
[3]*National Clinical Research Center for Oral Diseases, National Engineering Laboratory for Digital and Material Technology of Stomatology, Beijing 100081, China*
[4]*Key Laboratory of Cell Proliferation and Differentiation of the Ministry of Education, School of Life Sciences, Peking University, Beijing 100081, China*
[5]*Peking-Tsinghua Center for Life Sciences, Beijing 100081, China*
[6]*Central Laboratory, Peking University School and Hospital of Stomatology, Beijing 100081, China*

Correspondence should be addressed to Yunfei Zheng; yunfei_zheng@bjmu.edu.cn and Weiran Li; weiranli@bjmu.edu.cn

NOD-like receptor family pyrin domain-containing 3 (NLRP3) inflammasome is reportedly involved in periodontal pathogenesis. *Pasteurella multocida* toxin (PMT) is the major virulence factor of *Pasteurella multocida* strains, which belongs to the nonoral gram-negative facultative rods (GNFR). The existence of GNFR and their toxin may aggravate periodontitis. Therefore, it is important to unclose the regulatory mechanisms of PMT in periodontitis. However, the involvement of NLRP3 inflammasome and PMT in periodontitis remain unclear. The results showed that NLRP3 expression was increased in periodontitis mice by immunohistochemical staining and quantitative reverse transcription polymerase chain reaction (qRT-PCR). *Nlrp3*^{-/-} mice showed less periodontal bone loss and lower abundances of *Pasteurella multocida* by 16S rRNA sequencing. PMT promoted NLRP3 expressions by activating nuclear factor kappa light chain enhancer of B cells (NF-κB) pathway and activated NLRP3 inflammasome. This effect was reversed by NLRP3 inhibitor MCC950. Furthermore, PMT aggravated periodontal bone loss and inflammation in WT mice, while MCC950 attenuated periodontal bone loss and inflammation. The *Nlrp3*^{-/-} periodontitis models with PMT local injection showed less bone loss and inflammation compared with WT periodontitis mice after PMT treatment. Taken together, our results showed that PMT aggravates periodontal response to the ligature by promoting NLRP3 expression and activating NLRP3 inflammasome, suggesting that NLRP3 may be an effective target for the treatment of periodontitis caused by GNFR and MCC950 may be a potential drug against this disease.

1. Introduction

Periodontitis is a bacterial-induced chronic inflammatory disease resulting from an imbalance between bacterial antigens and host immune reactions [1, 2]. It affects about 50% of the global population, becoming the sixth most prevalent disease worldwide [3]. Inflammasome plays key roles innate immune system that rapidly recognizes and triggers the body's response to infections and potentially harmful foreign substances [4]. Several inflammasomes have been reported to be involved in the pathogenesis of periodontal disease [5]. For example, the gingival expression of NOD-like receptor family pyrin domain-containing 2 (NLRP2) inflammasomes were increased in periodontitis compared

with healthy controls [6]. In the gingiva of periodontitis patients, absent in melanoma 2 (AIM2) expression was significantly increased (S. [7]). NOD-like receptor family pyrin domain-containing 3 (NLRP3) inflammasome is one of the most important inflammasomes involved in the development of periodontitis. NLRP3 inflammasome is composed of NLRP3, apoptosis-associated speck-like protein containing a caspase recruitment domain (ASC), and pro-caspase-1. Two signals activate the NLRP3 inflammasome: an initial priming signal 1 and an activation signal 2. Priming signal 1 is initiated by toll-like receptor (TLR) activation, which subsequently activates the nuclear factor kappa light chain enhancer of B cells (NF-κB) pathway, thus inducing the expression of pro-IL-1β, pro-IL-18, and pro-caspase-1. Through activation signal 2, the NLRP3 protein clustering the ASC protein triggers oligomerization of pro-caspase-1, inducing cleavage to form the mature caspase-1 [8]. Active caspase-1 cleaves pro-IL-1β and pro-IL-18, inducing their activation and secretion and recruiting more effector cells to the infection site [9]. Therefore, activated IL-1β is one of important indicators of NLRP3 inflammasome activation. Recently, a study found that NLRP3 inflammasome mediated elder mice alveolar bone loss and that targeting NLRP3 inflammasome may be a novel option to control periodontal degeneration with age [10].

To date, there are conflicting reports on whether bacteria can activate NLRP3 inflammasome. Some studies found *Porphyromonas gingivalis* (*P.g.*) activates NLRP3 inflammasome through TLR2 and TLR4 pathways [11, 12]. By contrast, other studies suggested that *P.g.* inhibits the activation of NLRP3 inflammasomes and plays a counter-regulatory role [13]. Therefore, the role and underlying mechanisms of the NLRP3 inflammasome in periodontitis need further exploration. In present study, *in vivo* experiments revealed lower abundances of *Pasteurella multocida*, which belongs to the nonoral gram-negative facultative rods (GNFR), in *Nlrp3*^{-/-} mice than in WT mice. *Pasteurella multocida* infection induces NLRP3 inflammasome activation, and IL-1β secretion depends on NIMA-related kinase 7 (Nek7) and potassium efflux [14–16].

However, the association between *Pasteurella multocida* toxin (PMT), the major virulence factor of *Pasteurella multocida*, and NLRP3 inflammasome remain unclear. Therefore, the aim of the current study was to unclose the regulatory mechanisms of PMT and NLRP3 inflammasome in periodontitis, providing potential target for the treatment of periodontitis caused by GNFR.

2. Materials and Methods

2.1. Animals.
Male, 8-week-old, *Nlrp3*^{-/-} mice and wild-type (WT) C57BL/6 mice were used. *Nlrp3*^{-/-} mice were provided by the School of Life Sciences, Peking University (China). WT mice were purchased from WeiTong LiHua Co. (China). Animals were housed at the same time under the same specific-pathogen-free conditions.

2.2. Experimental Periodontitis and Treatment.
To build ligature-induced periodontitis model, sterile silk (5-0) was ligatured around the cervical areas of the upper right second molars of mice for one week. Interventions included local injection of the NLRP3 inhibitor MCC950 (MedChemExpress, Monmouth Junction, NJ, USA), 10 mg (5 μL) twice a day or of PMT (Proteintech Group, Rosemont, PA, USA), and 10 nM (5 μL) twice a day around the periodontal area. The control group was injected the same volume of normal saline (NS). The injections began on the day that the silks were ligatured (Figure S1). All animal experiments protocol was approved by the Experimental Animal Welfare Ethics Branch of Peking University Biomedical Ethics Committee (Protocol LA2020329) and complied with the ARRIVE guideline.

2.3. Microbial Sample Collection and 16S Ribosomal RNA (rRNA) Sequencing and Analysis.
After ligature-induced periodontitis for seven days, the silk was removed and transferred into sterile Eppendorf tubes. Then, 200 μL of phosphate-buffered saline was added to each tube and shaken for 1 h. The samples were centrifuged at 4°C for 16S rRNA sequencing.

E.Z.N.A. DNA Kit (Omega Bio-tek, Norcross, GA, USA) was used to extract microbial genomic DNA according to the manufacturer's instructions. The V3–V4 hypervariable regions of the 16S rRNA gene were subjected to high-throughput sequencing by Beijing Allwegene Tech, Ltd. (China) using the Illumina MiSeq PE300 sequencing platform (Illumina, Inc., San Diego, CA, USA). Quantitative Insights into Microbial Ecology package (v1.2.1) was used for high-quality sequence extraction. UCLUST was used to classify a unique sequence set into an operational taxonomy unit under a 97% identity threshold. Student's *t*-test was used to calculate alpha- and beta-diversity. The Kruskal-Wallis test was used to determine the significance of categorical variables.

2.4. Cell Preparation and Stimulation.
Human monocytes THP-1 were purchased from ScienCell (Carlsbad, CA, USA) and were cultured in RPMI 1640 supplemented with 10% fetal bovine serum (FBS, Gibco, Grand Island, NY, USA), 100 U/mL penicillin, and 100 μg/mL streptomycin at 37°C with 5% CO_2. THP-1 cells were differentiated into macrophage-like cells with 50 ng/mL of phorbol 12-myristate 13-acetate (PMA). The PMA-differentiated THP-1-derived macrophages were stimulated with different concentrations of PMT (0.1, 1, and 10 nM) for 6, 12, 24, 36, and 48 h.

2.5. DNA Extraction.
Genomic DNA were extracted by using the DNA DNeasy PowerSoil Pro Kits (QIAGEN, Dusseldorf, Germany) according to manufacturer's instruction. Briefly, the silk containing microbiota and Solution CD1 were added into the PowerBead Pro Tubes and horizontally vortex at maximum speed for 10 min. Then the PowerBead Pro Tubes were centrifuged at 15,000 g for 1 min. The supernatants were transfer to a clean 2-mL tube with 200 μL Solution CD2. The mixture was centrifuge at 15,000 g for 1 min, and the supernatants were transferred to another clean 2-mL tubes. 600 μL of Solution CD3 was added, and the whole

lysate were centrifuged through an MB Spin Column at 15,000 g for 1 min. Then 500 μL of Solution EA and 500 μL of Solution C5 were centrifuged through the MB Spin Column in order. Finally, 50 μL of Solution C6 was added to the center of the white filter membrane for centrifugation, and 16S rRNA genes from the extracted DNA were quantified by quantitative reverse transcription polymerase chain reaction (qRT-PCR). The primers for *Pasteurella multocida* and the internal control 16S rDNA are listed in Table S1.

2.6. qRT-PCR. Total RNA was extracted from the cells and periodontal tissues (gingival tissues and alveolar bone). Gingival tissues around the second molars were collected as gingival samples. Alveolar bone was collected after extraction of the second molar. TRIzol reagent (Invitrogen, Carlsbad, CA, USA) was added into these periodontal tissues to fully ground them. Then the procedure was as same as the RNA extraction procedure of cells, which was preformed according to previous study [17]. qRT-PCR was conducted using SYBR Green Master Mix (Roche Applied Science, Switzerland) on an ABI Prism 7500 Real-Time PCR System (Applied Biosystems, Foster City, CA, USA). The mean of housekeeping gene glyceraldehyde-3-phosphate dehydrogenase (GAPDH) was served as an internal reference. Results were calculated using the $2^{-\Delta\Delta Ct}$ relative expression method. The nucleotide sequences of the primers are listed in Table S1.

2.7. Western Blot. Total protein was extracted using radio immunoprecipitation assay lysis buffer supplemented with a protease inhibitor mixture. Protein concentrations were measured using Pierce BCA Protein Assay Kit (Thermo Scientific, Waltham, MA, USA), and equal amounts of proteins were separated by sodium dodecyl sulfate-polyacrylamide gel electrophoresis and then transferred onto polyvinylidene fluoride membranes (Millipore, Boston, MA, USA). Primary antibodies against NLRP3 (1:1,000, Proteintech Group), phosphorylated-p65 (1:1,000, Cell Signaling Technology, USA), p65 (1:1,000, Proteintech Group), IκBα (1:1000, Proteintech Group), and β-actin (1:2,000, ZSGB-Bio, Beijing, China) were incubated overnight at 4°C. The corresponding secondary antibodies (1:10,000, ZSGB-Bio) were incubated the next day for 1 h. The intensities of the bands obtained were quantified using ImageJ software (http://rsb.info.nih.gov/ij/) [18]. The signals of the target bands were normalized to the β-actin band relative to the control groups.

2.8. Microcomputed Tomography (Micro-CT). To analyze periodontal bone loss after ligation, the fixed mice maxillae were scanned using a SkyScan 1174 micro-CT system (Bruker, Kontich, Belgium) at a resolution of 10.8 μm. NRecon and CTvox software were used for three-dimensional (3D) reconstruction. Bone volume (BV), bone mineral density (BMD), and bone volume/tissue volume (BV/TV) ratio were calculated using the CTAn software (gray value >1000) by extracting all teeth on the CT data of region of interests according to previous study [19]. The distance between the cemento-enamel junction (CEJ) and the alveolar bone crest (ABC) from each side of the upper second molar (mesial, distal, lingual, and buccal sides) was measured on the sagittal and coronal planes using Data Viewer software.

2.9. Histological Analysis of Periodontal Tissue. The specimens (5 μm sections) were stained with hematoxylin and eosin (H&E) staining kit (G1120, Solarbio, Beijing, China). For immunohistochemical staining, the sections were rehydrated in a graded ethanol series and incubated with an antigen retrieval solution (C1034, Solarbio) for 15 min at 95°C. Then, sections were incubated with 3% hydrogen peroxide for 10 min at room temperature and incubated with primary antibodies against NLRP3 (1:800, Servicebio, Wuhan, China) and IL-1β (1:800, Servicebio) overnight at 4°C. Secondary antibodies (ZSGB-Bio) were subsequently applied. After the production of a brown precipitate using a DAB detection kit (Sigma, St. Louis, MO, USA), the sections were counterstained with hematoxylin. Average optical density (integrated optical density (IOD)/area, AOD) were calculated to analyze the optical density of per unit area in the 400× magnification field.

2.10. Statistical Analyses. SPSS version 19.0 (IBM, Chicago, IL, USA) was used for statistical analyses. All data are expressed as the mean ± SD of at least three independent experiments. A two-tailed unpaired Student's t-test was used for two-group comparisons. One-way analysis of variance (ANOVA) was used for multiple group comparisons. The threshold of statistical significance was set at $P < 0.05$.

3. Results

3.1. NLRP3 Expression Is Upregulated in Periodontitis Mice. We first build periodontitis mice model and the H&E staining and micro-CT results showed that ligature-induced periodontitis had been successfully constructed (Figures 1(a) and 1(c)). BV, BV/TV, and BMD were lower in the periodontal group than in the control group (Figure 1(b)). The distances from cemento-enamel junction (CEJ) to alveolar bone crest (ABC) of the mesial side was greater in the periodontal group than in the control group (Figure 1(d)). The mRNA levels of NLRP3, IL-1β, and IL-6 from alveolar bone and gingival tissues were significantly higher in the diseased group than in the control group (Figure 1(e)). Similarly, immunohistochemistry and semiquantitative analysis (integrated optical density (IOD)/area) results revealed a higher expression of IL-1β and NLRP3 in the gingival tissues of mice with periodontitis than in the healthy gingivae of WT mice (Figure 1(f)).

3.2. NLRP3 Deficiency Attenuates Mice Ligatured-Induced Periodontal Bone Loss and Inflammation In Vivo. WT ($n = 5$) and *Nlrp3*$^{-/-}$ ($n = 5$) mice were used to explore the role of NLRP3 in the development of ligature-induced periodontitis. *Nlrp3*$^{-/-}$ mice showed less bone loss than WT mice (Figure 2(a)). The distances between the CEJ and ABC from the mesial side were less in *Nlrp3*$^{-/-}$ mice than in WT mice (Figure 2(b)). BMD, BV, and BV/TV were higher in *Nlrp3*$^{-/-}$ mice than in WT mice (Figure 2(c)). Consistently, H&E staining results showed inflammation, and bone resorption
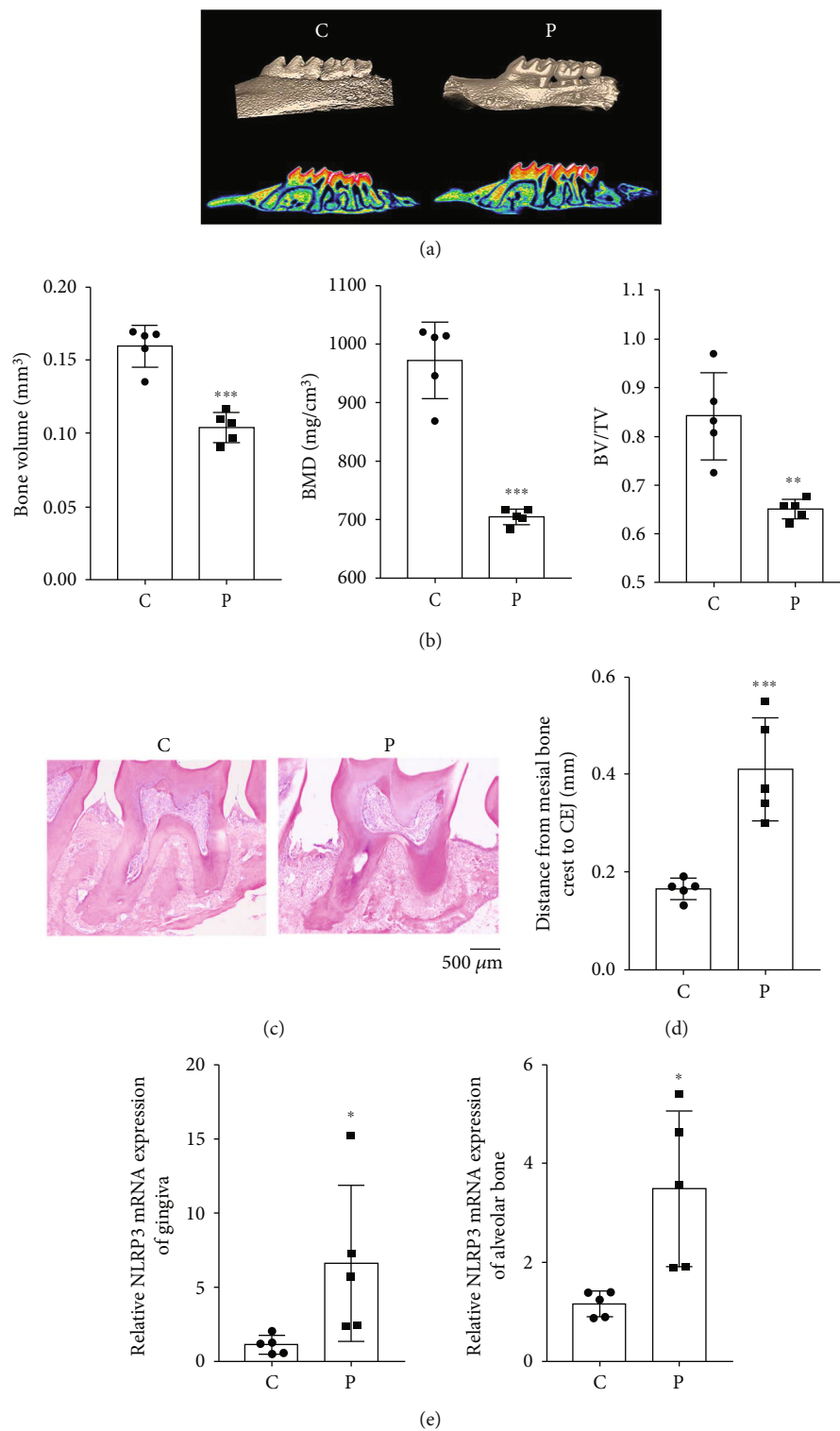
(a)

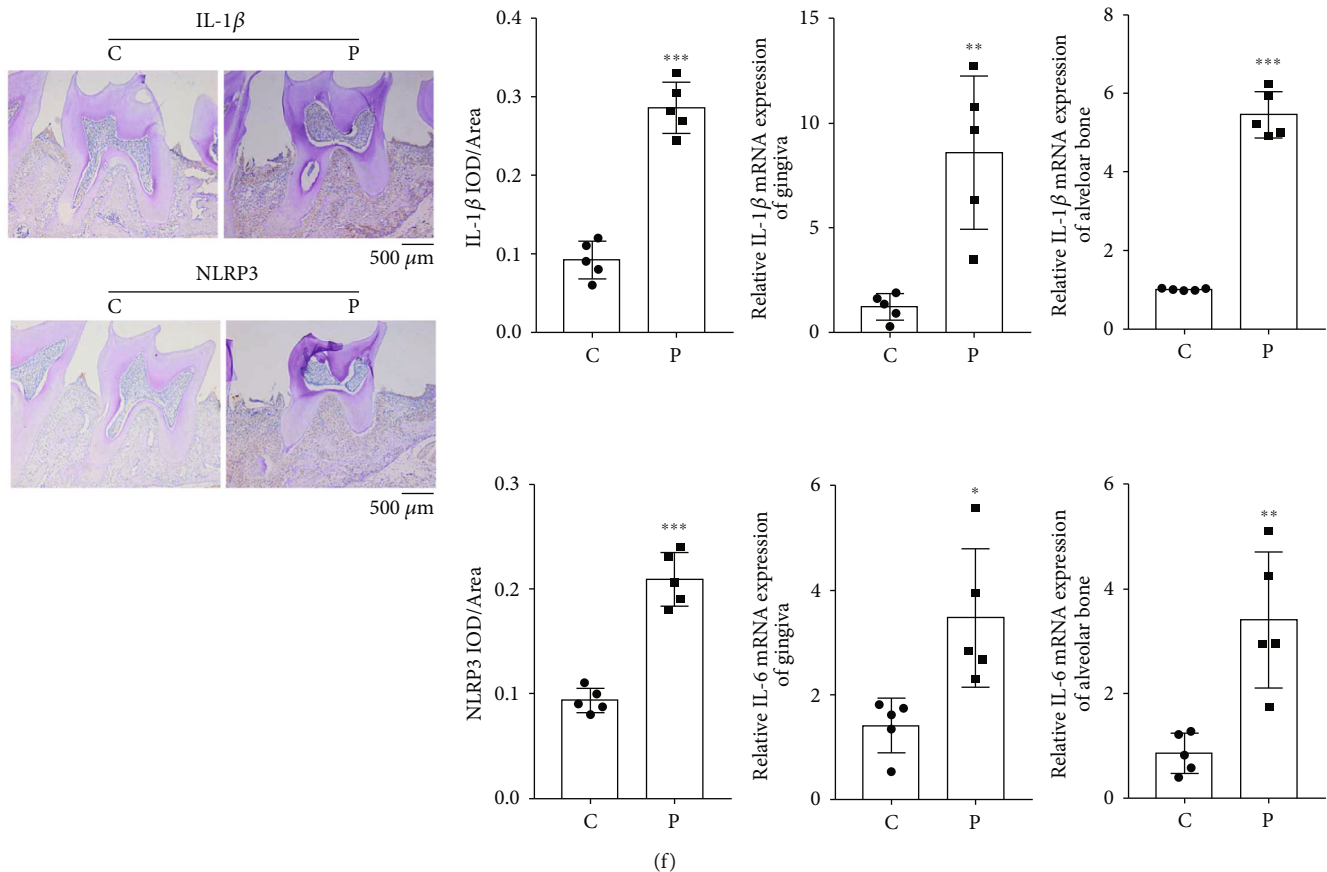

(b)

(c)

(d)

(e)

Figure 1: Continued.

FIGURE 1: NLRP3 expression is upregulated in periodontitis patients and mice. (a) Reconstructed 3D micro-CT images of the control and periodontitis groups. (b) BV, BV/TV, and BMD analysis of the control and periodontitis groups ($n = 5$/group). (c and f) H&E staining and immunohistochemistry staining of IL-1β and NLRP3 in the gingivae in control and periodontitis groups. Semiquantitative analysis (integrated optical density (IOD)/area) of IL-1β and NLRP3 immunohistochemistry staining of control and periodontitis groups. Values are presented as mean ± SD. (d) The distances between the CEJ and the ABC from the mesial side of the control and periodontitis groups ($n = 5$/group). (e) mRNA expression of IL-1β, IL-6, IL-10, and NLRP3 in the control and periodontitis groups by qRT-PCR ($n = 5$/group). GAPDH was used for normalization relative to control groups (*$P < 0.05$, **$P < 0.01$, and ***$P < 0.001$). Abbreviations: ABC = alveolar bone crest; BMD = bone mineral density; BV = bone volume; BV/TV = bone volume/tissue volume ratio; CEJ = cemento-enamel junction; GAPDH = glyceraldehyde-3-phosphate dehydrogenase; H&E = hematoxylin and eosin; IL = interleukin; micro-CT = microcomputed tomography; mRNA = messenger RNA; NLRP3 = NOD-like receptor family pyrin domain-containing 3; qRT-PCR = quantitative reverse transcription polymerase chain reaction; 3D = three-dimensional.

were significantly attenuated in $Nlrp3^{-/-}$ mice (Figure 2(d)). Moreover, NLRP3 deficiency remarkably decreased the mRNA expression of the inflammatory cytokines IL-1β and IL-6 (Figure 2(e)). Immunohistochemistry results further confirmed that NLRP3 deficiency significantly reduced IL-1β expression in gingival tissues of $Nlrp3^{-/-}$ mice than in those of WT mice (Figures 2(f) and 2(g)).

3.3. Altered Oral Microbiota between WT and Nlrp3$^{-/-}$ Mice. Previous study reported that NLRP3 knockout increase the capability of macrophage phagocytosis [20]. Therefore, we hypothesized that whether NLRP3 inflammasome influence the oral microbiota, which further influence the progression of periodontitis. Oral microbiota from the silk were collected to analyze the differences in oral bacterial communities between WT ($n = 3$) and $Nlrp3^{-/-}$ mice ($n = 3$) with ligature-induced periodontitis. 16S rRNA gene sequencing analysis revealed that despite individual variations in microbiota, a

general discrete clustering pattern of bacterial taxa was depicted between WT and $Nlrp3^{-/-}$ mice based on a principal component analysis (Figure 3(a)). The most significant difference in the microbial abundance between WT and $Nlrp3^{-/-}$ mice was $Pasteurella$ at the genus level, which was rare in $Nlrp3^{-/-}$ mice and enriched in WT mice. To further validate the differentially abundant species we identified according to our 16S rRNA-based microbiome analysis, we used qRT-PCR to quantify the presence of $Pasteurella multocida$. The results showed that the fold changes of $Pasteurella multocida$ in $Nlrp3^{-/-}$ periodontitis mice were significantly less compared with the WT periodontitis mice (Figure 3(b)). The relative abundance analysis results were also consistent with the 16S rRNA gene sequencing analysis (Figure 3(b)).

3.4. PMT Induces Transcription and Expression of NLRP3 and Inflammatory Reaction In Vitro. We then explored the potential influence of PMT, the major virulence factor of
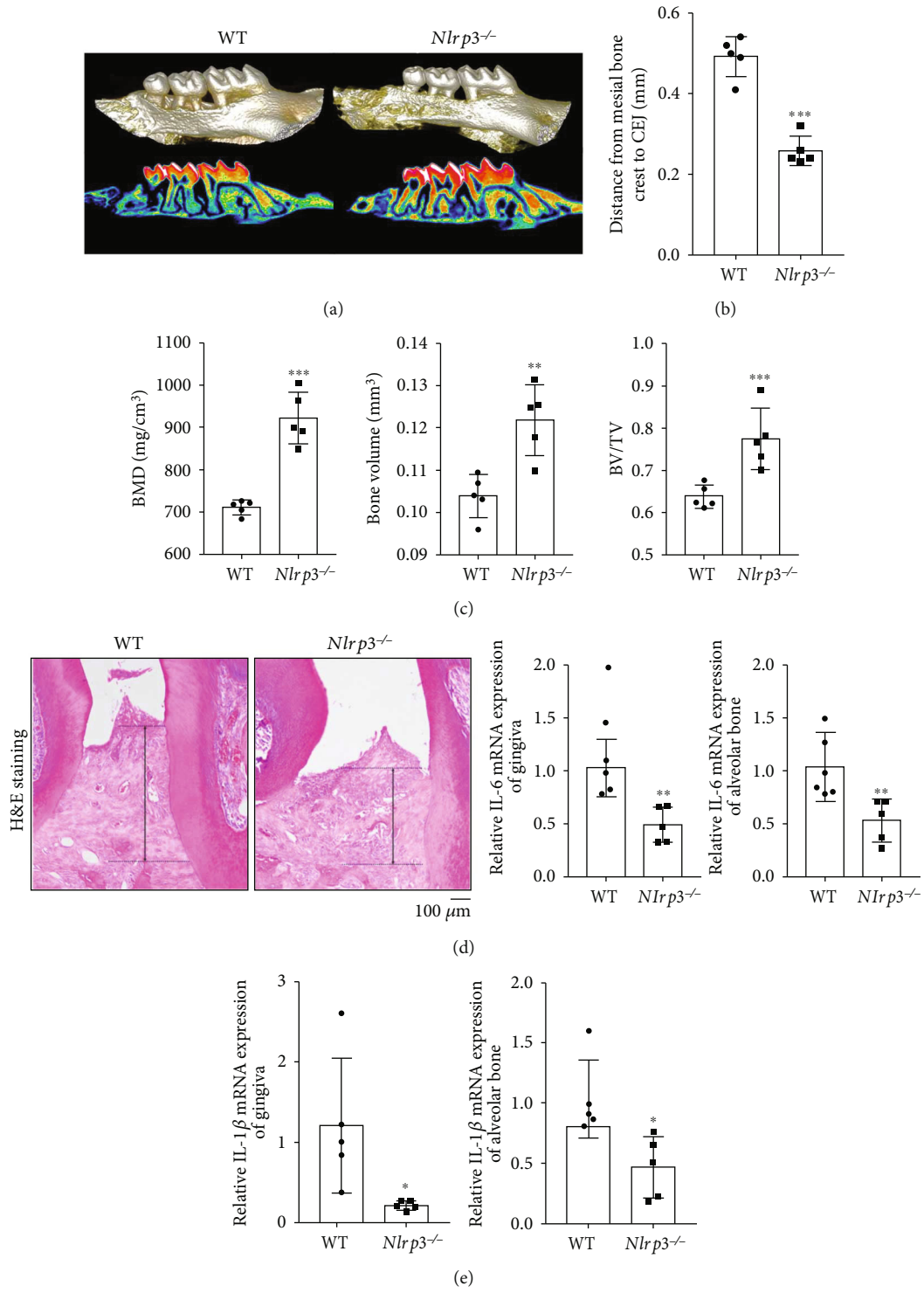
(a)

(b)

(c)

(d)
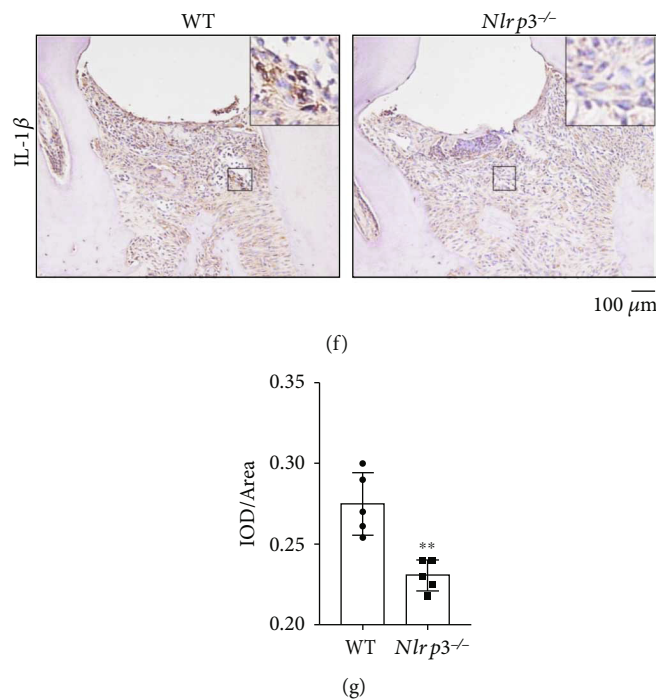
(e)

Figure 2: Continued.

(f)

(g)

FIGURE 2: NLRP3 deficiency attenuates mice periodontitis *in vivo*. (a) Reconstructed 3D micro-CT images of periodontitis models of WT and *Nlrp3*$^{-/-}$ mice. (b) The distances between the CEJ and the ABC from the mesial side of upper right second molars of WT and *Nlrp3*$^{-/-}$ mice ($n = 5$/group). (c) BMD, BV, BV/TV, and resorbed bone volume analysis of WT and *Nlrp3*$^{-/-}$ mice ($n = 5$/group). (d, f, and g) H&E staining and immunohistochemistry staining of IL-1β of WT and *Nlrp3*$^{-/-}$ mice. The histogram shows the quantification of average optical density (integrated optical density (IOD)/area) of IL-1β immunohistochemistry staining of WT and *Nlrp3*$^{-/-}$ mice groups ($n = 5$/group). (e) mRNA expression of IL-1β and IL-6 in the gingiva and alveolar bone of WT and *Nlrp3*$^{-/-}$ mice ($n = 5$/group) by qRT-PCR. GAPDH was used for normalization relative to control groups. Values are presented as mean ± SD ($^*P < 0.05$, $^{**}P < 0.01$, and $^{***}P < 0.001$). Abbreviations: ABC = alveolar bone crest; BMD = bone mineral density; BV = bone volume; BV/TV = bone volume/tissue volume ratio; CEJ = cemento-enamel junction; GAPDH = glyceraldehyde-3-phosphate dehydrogenase; H&E = hematoxylin and eosin; IL = interleukin; micro-CT = microcomputed tomography; mRNA = messenger RNA; NLRP3 = NOD-like receptor family pyrin domain-containing 3; qRT-PCR = quantitative reverse transcription polymerase chain reaction; 3D = three-dimensional.

Pasteurella multocida on the progression of periodontitis, and investigated whether PMT has an impact on periodontitis via the NLRP3 inflammasome. The mRNA expression of IL-1β, IL-6, and NLRP3 were all significantly upregulated after the stimulation of PMT as well as tumor necrosis factor (TNF), which is an NF-κB pathway agonist in a time- and dose-dependent manner (Figure 3(c), Figure S2A-C) [21]. As the mRNA expression of NLRP3 reached the highest peak at 12 h with 10 nM of both PMT and TNF, we chose 12 h as the stimulation time and 10 nM as the dose in further experiments. Consistently, western blot results also confirmed that PMT exposure induced the protein expression of NLRP3. Similarly, the protein expression of NLRP3 reached the highest peak at 12 h (Figure 3(d), Figure S2D). We further found that PMT activated the NF-κB signaling pathway and the application of NF-κB inhibitor Bay 11-7082 attenuated PMT-induced NF-κB signaling pathway activity (Figure 3(e)).

3.5. *PMT Activates NLRP3 Inflammasome In Vitro*. We next explored whether PMT participated in the NLRP3 inflammasome activation process. Western blot results showed PMT activated NLRP3 inflammasome with the activation of caspase-1 and the release of activated IL-1β

(Figure 4(a)). However, this effect was significantly inhibited using the NLRP3 inhibitor MCC950 in a dose-dependent manner. Pretreatment with 1 μM MCC950 for 1 h had a minimal effect on PMT-induced NLRP3 inflammasome activation, whereas pretreatment with 10 μM MCC950 significantly reduced the release of activated IL-1β in both whole cell lysates and culture supernatants (Figure 4(b)). Additionally, MCC950 did not affect NLRP3 protein expression but inhibited NLRP3 inflammasome activation. Furthermore, the time of MCC950 effect against PMT via NLRP3 inhibition was limited. Pretreatment with 10 μM MCC950 significantly reduced the release of activated IL-1β in both whole cell lysates and culture supernatants after 12 h of PMT stimulation. However, MCC950 rarely inhibited NLRP3 inflammasome expression after PMT stimulation for 24 h (Figure 4(c)). The regulatory mechanism is deduced in Figure 4(d), and the flow chart of the whole experiment was shown in Figure S3.

3.6. *MCC950 Ameliorates Mice Periodontal Response to the Ligature while PMT Aggravates Mice Periodontal Response to the Ligature*. Next, we explore the role of MCC950 and PMT on the progression of periodontitis *in vivo*. Micro-CT reconstruction results demonstrated that MCC950 ameliorated
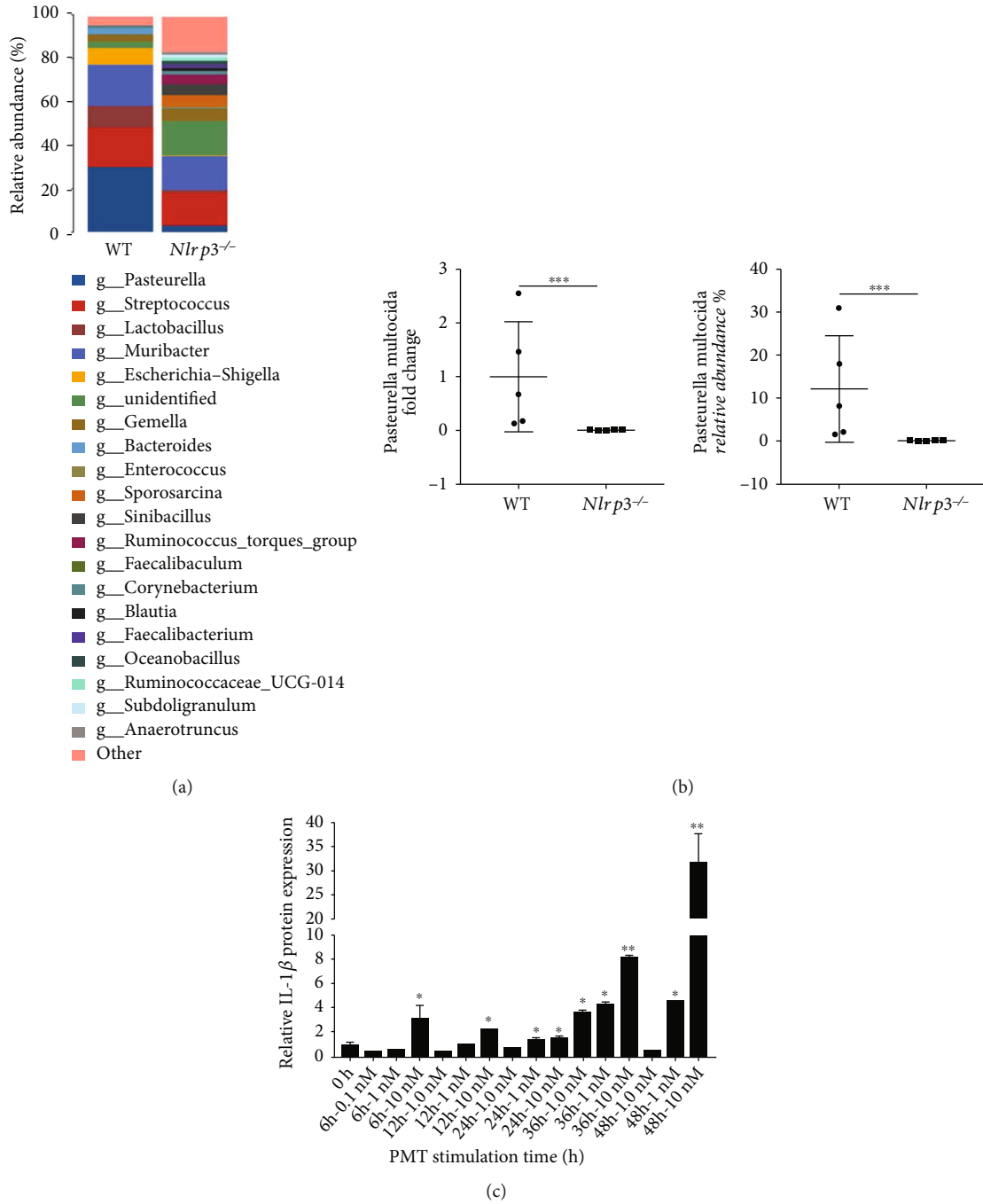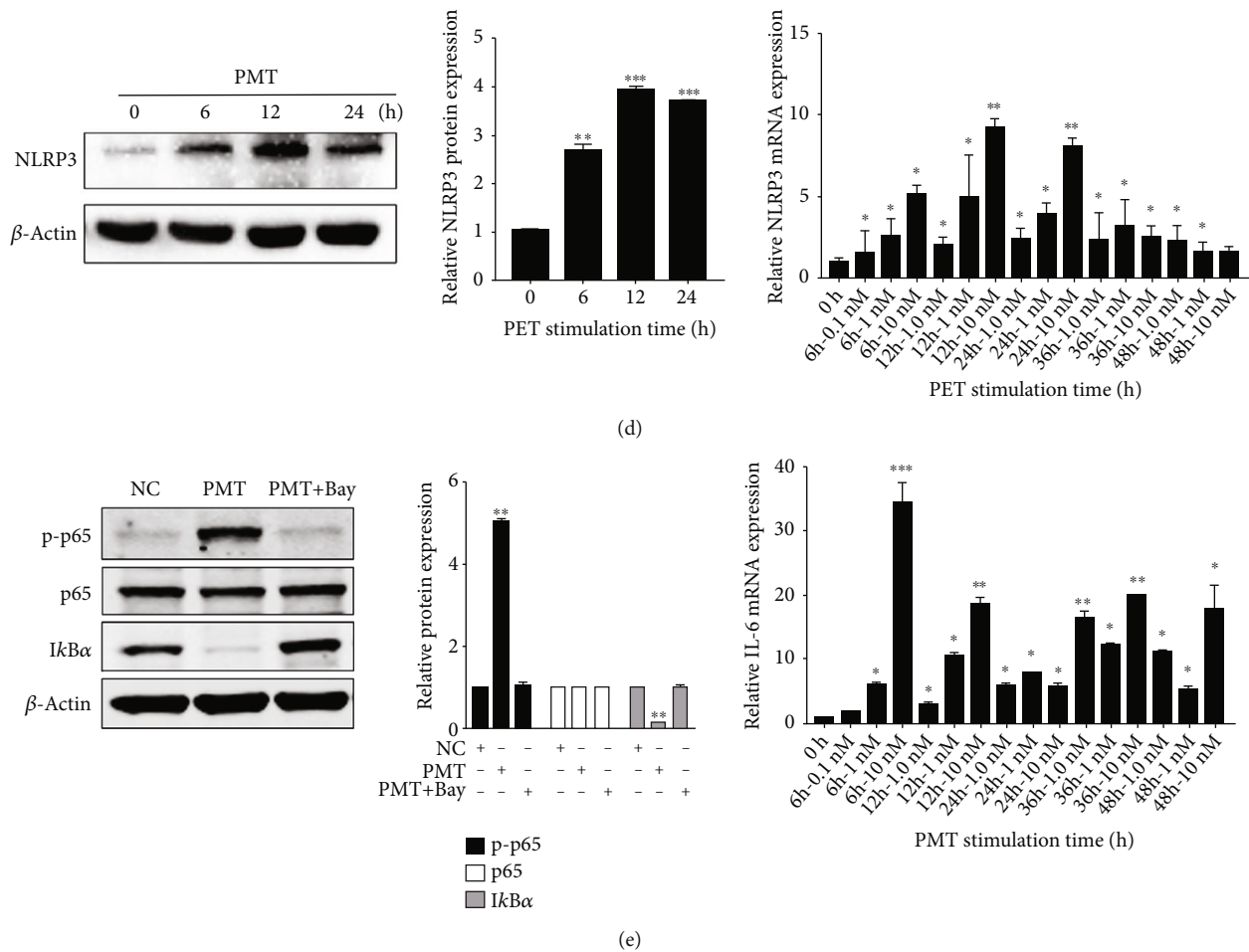
(a)

(b)

(c)

Figure 3: Continued.

(d)

(e)

FIGURE 3: Altered oral microbiota between WT and $Nlrp3^{-/-}$ mice and PMT induces transcription and expression of NLRP3 and inflammatory reaction *in vitro*. (a)16S rRNA gene sequencing analysis show the general discrete clustering pattern of bacterial taxa between WT and $Nlrp3^{-/-}$ mice ($n = 3$/group). (b) qRT-PCR validation of *Pasteurella multocida* in WT and $Nlrp3^{-/-}$ mice ($n = 5$/group). (c) mRNA expression of IL-1β, IL-6, and NLRP3 after the stimulation of PMT at a series of time by qRT-PCR ($n = 5$/group). GAPDH was used for normalization relative to control groups. (d) Protein expression of NLRP3 and the internal control β-actin after the stimulation of PMT at a series of time by western blot. The histogram shows the quantification of band intensities. β-Actin was used for normalization relative to the control groups. (e) Protein expression of pp65, p65, IκBα, and the internal control β-actin after stimulation of PMT with or without pretreatment of NF-κB inhibitor Bay 11-7082 by western blot. The histogram shows the quantification of band intensities. β-Actin was used for normalization relative to the control groups. Values are presented as mean ± SD ($^{*}P < 0.05$, $^{**}P < 0.01$, and $^{***}P < 0.001$). Abbreviations: GAPDH = glyceraldehyde-3-phosphate dehydrogenase; IL = interleukin; mRNA = messenger RNA; NLRP3 = NOD-like receptor family pyrin domain-containing 3; NF-κB = nuclear factor kappa light chain enhancer of B cells; PMT = *Pasteurella multocida* toxin; qRT-PCR = quantitative reverse-transcription polymerase chain reaction.

ligature-induced periodontitis, as PMT aggravated ligature-induced periodontitis (Figure 5(a)). MCC950 treatment significantly improved periodontal bone resorption and inflammation. The ligature-induced periodontitis group synchronously treated with PMT showed a more severe bone loss than the untreated ligature-induced periodontitis group (Figure 5(b)). Similarly, both H&E staining and software analysis calculating the distances between the CEJ and ABC from the mesial side showed consistent results (Figure 5(c)). Immunohistochemical staining results showed that IL-1β expression was significantly higher in the PMT treatment group, while was significantly lower in the MCC950 injection group (Figure 5(d)). Moreover, we detected the relative expression of *Pasteurella multocida* and found that the fold changes of *Pasteurella multocida* in

ligature-induced periodontitis mice after MCC950 treatment were less compared with the WT periodontitis mice group (Figure S4A). And the abundance of *Pasteurella multocida* relative to the total bacteria in ligature-induced periodontitis mice after MCC950 treatment were also less compared with the WT periodontitis mice group (Figure S4B).

3.7. PMT Aggravates Periodontitis Progression via NLRP3 Inflammasome. Then WT and $Nlrp3^{-/-}$ mice were used to further verify whether PMT aggravates periodontitis progression via NLRP3 inflammasome. With local injection of PMT, $Nlrp3^{-/-}$ mice showed less bone loss compared to the WT periodontitis mice (Figure S5A, B). H&E staining results demonstrated that the perpendicular distance from
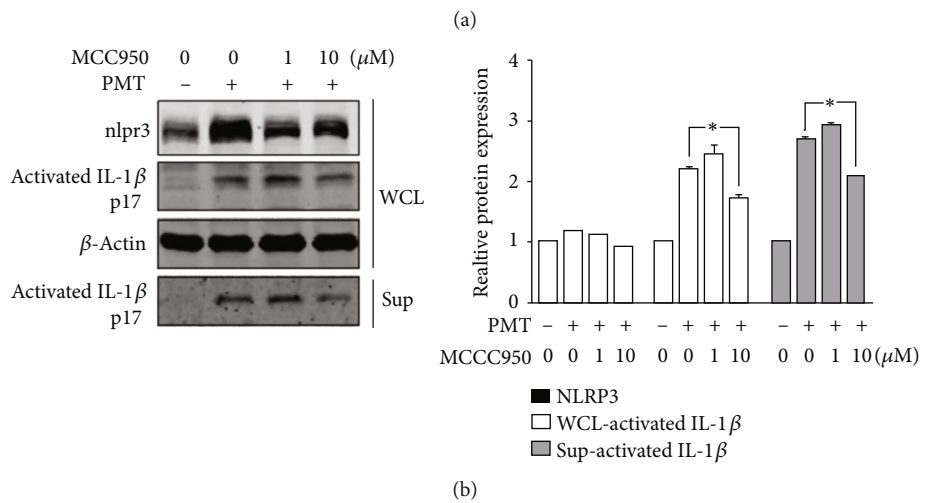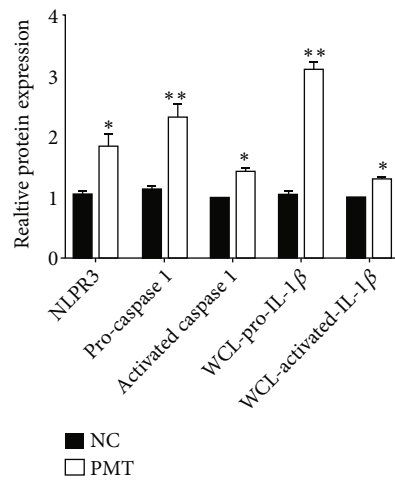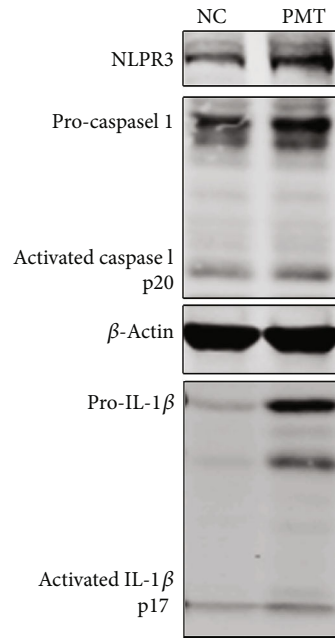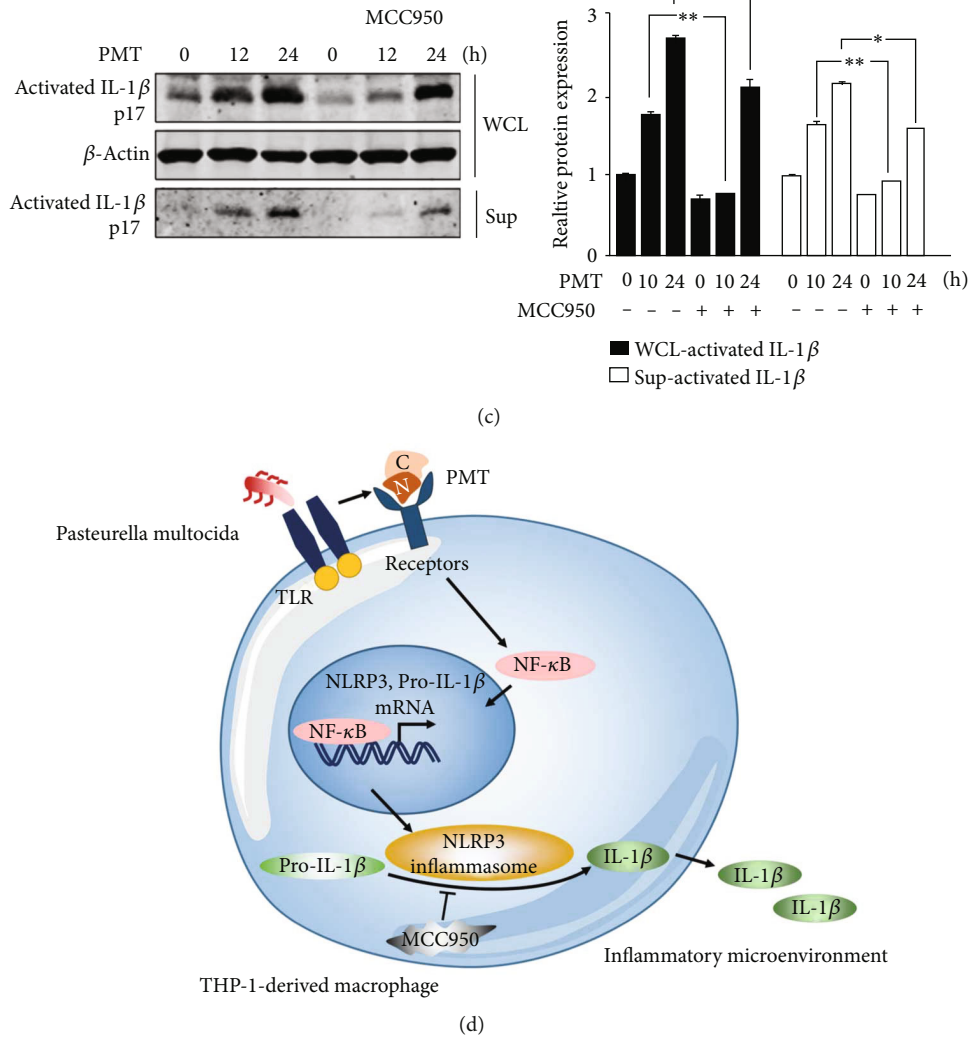
(a)

(b)

Figure 4: Continued.

(c)

(d)

FIGURE 4: PMT activates NLRP3 inflammasome *in vitro*. (a) Protein expression of NLRP3, pro-caspase-1, activated caspase-1, pro-IL-1β, activated IL-1β, and the internal control β-actin after stimulation of PMT for 12 h by western blot. The histogram shows the quantification of band intensities. β-Actin was used for normalization relative to the control groups. (b) Protein expression of NLRP3, pro-IL-1β, activated IL-1β in whole cell lysates and supernatants, and the internal control β-actin after stimulation of PMT with or without NLRP3 inhibitor MCC950 by western blot. The histogram shows the quantification of band intensities. β-Actin was used for normalization relative to the control groups. (c) Protein expression of activated IL-1β in whole cell lysates (WCL) and supernatants (Sup) and the internal control β-actin after stimulation of PMT with or without NLRP3 inhibitor MCC950 in a series of time by western blot. The histogram shows the quantification of band intensities. β-Actin was used for normalization relative to the control groups. (d) Diagram illustrated that PMT can not only induce inflammatory reactions and the transcription of NLRP3 via the NF-κB signaling pathway but also activate NLRP3 inflammasome with the release of activated IL-1β. NLRP3 inhibitor MCC950 can significantly reduce this effect. Values are presented as mean $\pm$ SD ($^{*}P < 0.05$ and $^{**}P < 0.01$). Abbreviations: IL = interleukin; mRNA = messenger RNA; NLRP3 = NOD-like receptor family pyrin domain-containing 3; NF-κB = nuclear factor kappa light chain enhancer of B cells; PMT = *Pasteurella multocida* toxin.

the mesial and distal ABC to the CEJ was less in *Nlrp3*$^{-/-}$ mice than in the WT periodontitis mice (Figure S5A, C), suggesting PMT aggravates periodontitis progression via NLRP3 inflammasome.

4. Discussion

Patients with periodontitis showed higher levels of NLRP3 in the gingival crevicular fluid, indicating the important role of NLRP3 in periodontitis progression [22]. NLRP3 inflamma-

some recognizes various stimuli, such as pathogen-associated molecular patterns and endogenous damage-associated molecular patterns [23]. Periodontal pathogens including *P.g.*, *Aggregatibacter actinomycetemcomitans* (*A.a.*), and *Fusobacterium nucleatum* (*F.n.*) have been reported to activate the NLRP3 inflammasome, inducing IL-1β secretion [24–26]. Yamaguchi et al. found that *Nlrp3*$^{-/-}$ mice showed less alveolar bone resorption with oral *P.g.* injection compared with WT mice [27] indicating that NLRP3 inflammasome is involved in bone metabolism and resorption induced by *P.g.* infection.
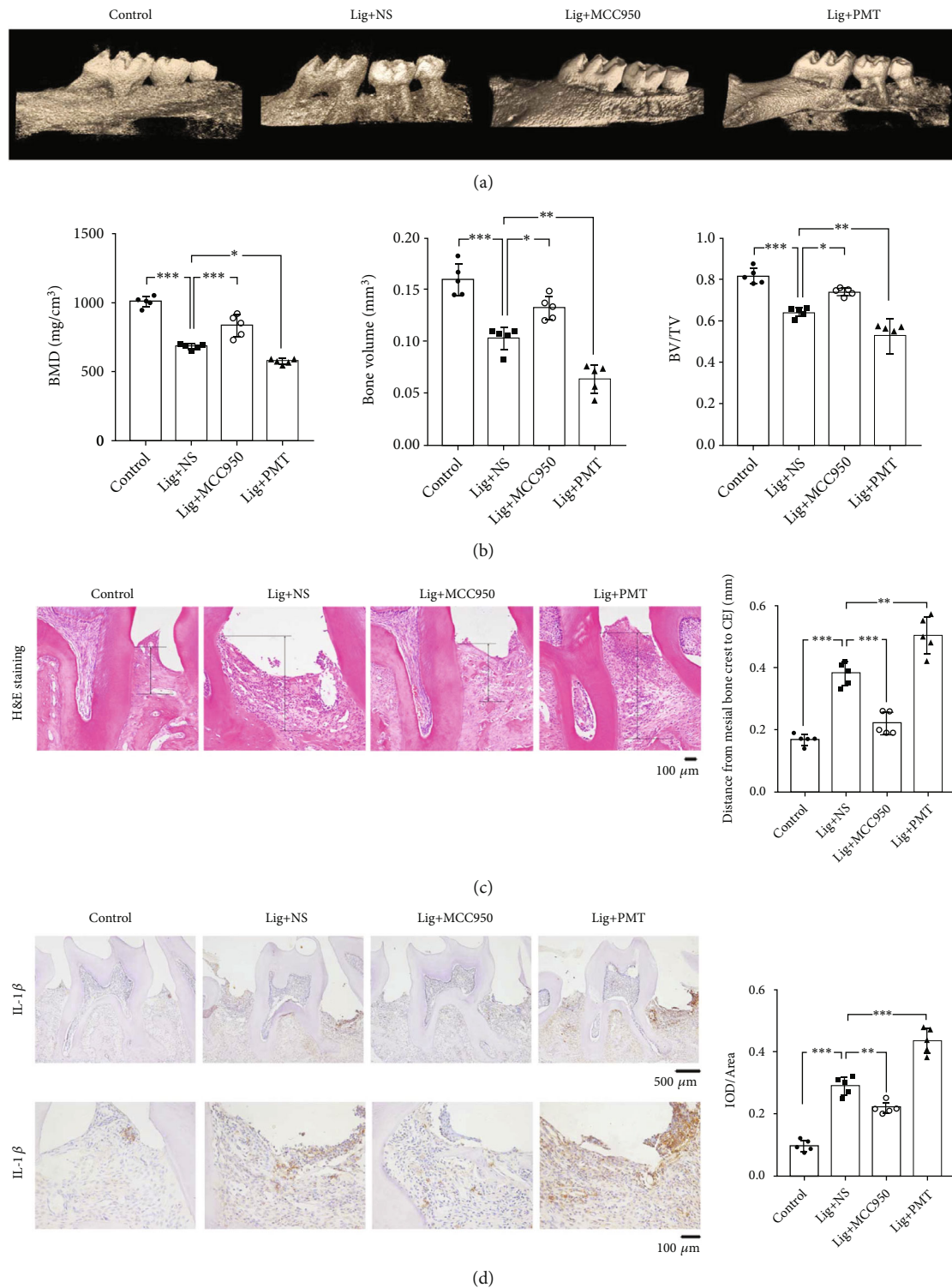
(a)

(b)

(c)

(d)

FIGURE 5: MCC950 ameliorates mice periodontitis, while PMT aggravates mice periodontitis. (a) Reconstructed 3D micro-CT images of the control, lig+NS, lig+MCC950, and lig+PMT groups. (b) BMD, BV, and BV/TV analysis of control, lig+NS, lig+MCC950, and lig+PMT groups. (c) H&E staining and the distances between the CEJ and the ABC from mesial side of f control, lig+NS, lig+MCC950, and lig+PMT groups. (d) Immunohistochemistry staining of IL-1β in the gingivae of the control, lig+NS, lig+MCC950, and lig+PMT groups. The histogram shows the quantification of average optical density (integrated optical density (IOD)/area) of IL-1β immunohistochemistry staining (n = 5/group). Values are presented as mean ± SD (*P < 0.05, **P < 0.01, and ***P < 0.001). Abbreviations: ABC=alveolar bone crest; BMD=bone mineral density; BV=bone volume; BV/TV=bone volume/tissue volume ratio; CEJ=cemento-enamel junction; H&E = hematoxylin and eosin; IL=interleukin; micro-CT=microcomputed tomography; NS=normal saline; PMT=*Pasteurella multocida* toxin; 3D=three-dimensional.

Consistently, in our study, NLRP3 expression was higher in ligature-induced periodontitis mice. Moreover, NLRP3 deficiency decreased ligature-induced periodontal bone tissue loss and inflammation.

In present study, we used 16S rRNA gene sequencing to detect the oral microbiota after ligature-induced periodontitis for seven days and the results showed that the most significant difference in the microbial abundance between WT and $Nlrp3^{-/-}$ mice was *Pasteurella* at the genus level. *Pasteurella multocida* is one of the most frequently isolated subgingival nonoral GNFR [28]. It is a commensal bacterium in the gingival crevice of BALB/c mice, nonhuman primates, ferret, and dog models [29–32]. At present, most periodontal therapies focus on major periodontopathogens such as *P.g.* and *A.a.* Though GNFR are not always inhabiting the human oral cavity, the existence of GNFR and their toxin may resist mechanical debridement from periodontal pockets and are insusceptible to most antibiotics frequently applied in periodontal treatment, even aggravate periodontitis. One of GNFR Neisseria has been reported to be a nitrate-reducing bacteria, promoting endothelial dysfunction, and increased cardiovascular risk [33]. However, the effects of GNFR in the progression of periodontitis remain largely unknown. *Pasteurella multocida* is conserved with *A.a.* and *Haemophilus influenzae*, all belonging to the phylogeny of the *Pasteurellaceae* group. PMT, the major virulence factor produced *by Pasteurella multocida* serotypes A and D strains [34], can lead to various pathological processes [35, 36]. One study reported that *A.a.*-immunized mice harboring *Pasteurella* in the oral cavity developed severe periodontitis [31]. In present study, we found PMT significantly aggravated ligature-induced periodontitis *in vivo*. In this study, we did not explore the role of *Pasteurella multocida* in the progression of periodontitis. In future experiments, the function of *Pasteurella multocida* in the progression of periodontitis and the underlying mechanisms, whether *Pasteurella multocida* activates NLRP3 inflammasome like other periodontal pathogens, and through which signal 1 and signal 2, need to be investigated.

In contrast to lipopolysaccharide, PMT is an AB toxin that can activate the heterotrimeric G proteins Gaq, Ga13, and Gai through deamidation of a glutamine residue required for guanosine triphosphate hydrolysis [37]. A previous study showed PMT stimulates IL-β gene transcription by inducing NF-κB activation; PMT induces IL-1β maturation independent of the NLRP3 inflammasome but dependent on Granzyme A in macrophages [38]. Moreover, the study found this Granzyme A-dependent mechanism is specific for mice macrophages, while human macrophages require NLRP3 inflammasome activation. We found PMT promoted IL-1β and NLRP3 gene transcription via NF-κB pathway activation and stimulated IL-1β secretion via NLRP3 inflammasome activation in human macrophages. Additionally, studies have reported PMT participates in bone homeostasis. It can trigger nuclear factor kappa-B ligand (RANKL)-independent osteoclastogenesis and inhibit osteogenesis via G protein signaling activation [39, 40]. NLRP3 inflammasome has been involved in osteoclastogenesis through IL-1β, which promotes RANKL-induced osteoclast differentiation [41, 42]. NLRP3 inflammasome NLRP3 regulates alveolar bone loss in ligature-induced periodontitis by promoting osteoclastic differentiation, and targeting it also reduced age-related alveolar bone loss [10]. However, whether PMT mediates bone resorption via the NLRP3 inflammasome requires further exploration.

NLRP3 inflammasome was regulated by various factors in periodontitis model to provide therapeutic strategies for periodontitis. Active periodontal disease downregulates inflammasome regulators including pyrin-only proteins (POPs), CARD-only proteins (COPs), and tripartite motif family proteins (TRIMs), which may increase the activity of NLRP3 and IL-1β in periodontal disease [6]. *F.n.* plus adenosine triphosphate (ATP) increased IL-1β expression by upregulating NLRP3 and AIM2 and by downregulating inflammasome regulator TRIM16 and POP1 levels. However, *P.g.* in the presence of ATP downregulated NLRP3 and POP1 and did not influence the AIM2 inflammasome in human primary gingival fibroblast (HGFs) [43]. Bmi-1 was reported to negatively regulate TLR4-specific activation of the NLRP3 pathway in a mouse model of periodontitis [44]. Oral administration of glyburide significantly suppressed the infiltration of inflammatory cells and the number of osteoclasts in the alveolar bone via targeting the NLRP3 pathway in periodontal diseases [25]. Few NLRP3 inflammasome inhibitors or activators have been reported in regulating the pathogenesis of periodontitis. MCC950 was discovered as a selective small molecule inhibitor of NLRP3 inflammasomes and has been experimentally proven to be beneficial in the control of inflammation and metabolic diseases. MCC950 can directly interact with the NLRP3 NACHT domain to prevent the formation and maintenance of the NLRP3 inflammasome complex [45, 46]. Our experiments demonstrated that MCC950 treatment effectively inhibits PMT-induced NLRP3 inflammasome activation and further suppresses IL-1β production in a concentration-dependent manne*r in vitro*. However, MCC950 are high cost and short half-life, and the development of more potent agents will offer insights into immune-mediated periodontitis strategies in future [47].

In conclusion, we confirmed there were lower abundances of *Pasteurella multocida* in $Nlrp3^{-/-}$ periodontitis mice than in WT periodontitis mice. PMT not only promoted NLRP3 expressions by activating NF-?B signaling pathway, but also effectively activated NLRP3 inflammasome to further trigger pro-IL-1β cleavage *in vitro*. PMT aggravated ligatured-induced periodontal bone loss and inflammation via NLRP3 inflammasome, and this effect was significantly reversed by NLRP3 inhibitor MCC950 with reduced IL-1β activation. Our findings enriched the understanding of NLRP3 inflammasome in the presence of GNFR during periodontitis progression. Furthermore, our findings provided a possibility that targeting NLRP3 inflammasome can alleviate PMT-induced periodontitis and that MCC950 can be a novel option to control periodontal diseases.

Abbreviations

A.a.:	*Aggregatibacter actinomycetemcomitans*
ABC:	Alveolar bone crest
ANOVA:	Analysis of variance
ASC:	Apoptosis-associated speck-like protein containing a CARD
BI:	Bleeding index
BMD:	Bone mineral density
BV:	Bone volume
BV/TV:	Bone volume/tissue volume
CEJ:	Cementum-enamel junction
EDTA:	Ethylenediaminetetraacetic acid
ELISA:	Enzyme-linked immunosorbent assay
F.n.:	*Fusobacterium nucleatum*
GAPDH:	Glyceraldehyde-3-phosphate dehydrogenase
GNFR:	Nonoral gram-negative facultative rods
H&E:	Hematoxylin and eosin
IL:	Interleukin
IOD:	Integrated optical density
LPS:	Lipopolysaccharide
micro-CT:	Microcomputed tomography
mRNA:	Messenger RNA
NLRP2:	NOD-like receptor family pyrin domain-containing 2
NLRP3:	NOD-like receptor family pyrin domain-containing 3
NF-κB:	Nuclear factor kappa light chain enhancer of B cells
NS:	Normal saline
P.g.:	*Porphyromonas gingivalis*
PMA:	Phorbol 12-myristate 13-acetate
PMT:	*Pasteurella multocida* toxin
QIIME:	Quantitative insights into microbial ecology
qRT-PCR:	Quantitative reverse-transcription polymerase chain reaction
RANKL:	Nuclear factor kappa-B ligand
Sup:	Supernatants
TLR:	Toll-like receptor
TNF:	Tumor necrosis factor
WCL:	Whole cell lysates
3D:	Three-dimensional.

Data Availability

The authors confirm that all data underlying the findings are fully available without restriction. All relevant data are within the paper and its Appendix files.

Disclosure

A preprint has been presented in Research square according to the following link: https://www.researchsquare.com/article/rs-1461888/v1 [48].

Conflicts of Interest

The authors have no conflicts of interest relevant to this article.

Supplementary Materials

Appendix. Table S1: nucleotide sequence of primers used in qRT-PCR. Figure S1: schedule of the experiment. Figure S2: TNFα and PMT induce transcription and expression of NLRP3 and inflammatory reaction *in vitro*. Figure S3: flow chart of the experiment design. Figure S4: qRT-PCR validation of *Pasteurella multocida* in lig + NS and lig + MCC950 mice groups ($n = 5$/group). Figure S5: PMT aggravates periodontitis progression via NLRP3 inflammasome. *(Supplementary Materials)*

References

[1] H. Kuula, T. Salo, E. Pirila et al., "Local and systemic responses in matrix metalloproteinase 8-deficient mice during Porphyromonas gingivalis-induced periodontitis," *Infection and Immunity*, vol. 77, no. 2, pp. 850–859, 2009.

[2] P. E. Petersen and H. Ogawa, "The global burden of periodontal disease: towards integration with chronic disease prevention and control," *Periodontology 2000*, vol. 60, no. 1, pp. 15–39, 2012.

[3] N. X. West, "Living with periodontitis," *British Dental Journal*, vol. 227, no. 7, p. 537, 2019.

[4] M. Lamkanfi and V. M. Dixit, "The inflammasome turns 15," *Nature*, vol. 548, no. 7669, pp. 534-535, 2017.

[5] K. Aral, M. R. Milward, Y. Kapila, A. Berdeli, and P. R. Cooper, "Inflammasomes and their regulation in periodontal disease: a review," *Journal of Periodontal Research*, vol. 55, no. 4, pp. 473–487, 2020.

[6] K. Aral, E. Berdeli, P. R. Cooper et al., "Differential expression of inflammasome regulatory transcripts in periodontal disease," *Journal of Periodontology*, vol. 91, no. 5, pp. 606–616, 2020.

[7] S. Kim, M. H. Park, Y. R. Song, H. S. Na, and J. Chung, "Aggregatibacter actinomycetemcomitans-induced AIM2 inflammasome activation is suppressed by xylitol in differentiated THP-1 macrophages," *Journal of Periodontology*, vol. 87, no. 6, pp. e116–e126, 2016.

[8] X. Yang, H. Y. Chang, and D. Baltimore, "Autoproteolytic activation of pro-caspases by oligomerization," *Molecular Cell*, vol. 1, no. 2, pp. 319–325, 1998.

[9] F. Martinon, K. Burns, and J. Tschopp, "The inflammasome: a molecular platform triggering activation of inflammatory caspases and processing of proIL-β," *Molecular Cell*, vol. 10, no. 2, pp. 417–426, 2002.

[10] Y. Zang, J. H. Song, S. H. Oh et al., "Targeting NLRP3 Inflammasome reduces age-related experimental alveolar bone loss," *Journal of Dental Research*, vol. 99, no. 11, pp. 1287–1295, 2020.

[11] N. Bostanci, G. Emingil, B. Saygan et al., "Expression and regulation of the NALP3 inflammasome complex in periodontal diseases," *Clinical and Experimental Immunology*, vol. 157, no. 3, pp. 415–422, 2009.

[12] E. Park, H. S. Na, Y. R. Song, S. Y. Shin, Y. M. Kim, and J. Chung, "Activation of NLRP3 and AIM2 inflammasomes

by Porphyromonas gingivalis infection," *Infection and Immunity*, vol. 82, no. 1, pp. 112–123, 2014.

[13] D. J. Taxman, K. V. Swanson, P. M. Broglie et al., "_Porphyromonas gingivalis_ mediates inflammasome repression in polymicrobial cultures through a novel mechanism involving reduced endocytosis," *The Journal of Biological Chemistry*, vol. 287, no. 39, pp. 32791–32799, 2012.

[14] R. Fang, H. Du, G. Lei et al., "NLRP3 inflammasome plays an important role in caspase-1 activation and IL-1β secretion in macrophages infected with _Pasteurella multocida_," *Veterinary Microbiology*, vol. 231, pp. 207–213, 2019.

[15] R. Fang, G. Lei, J. Jiang et al., "High- and low-virulent bovine _Pasteurella multocida_ induced differential NLRP3 inflammasome activation and subsequent IL-1 β secretion," *Veterinary Microbiology*, vol. 243, article 108646, 2020.

[16] Y. Wang, Z. Zeng, J. Ran et al., "The critical role of potassium efflux and Nek7 in Pasteurella multocida-induced NLRP3 inflammasome activation," *Frontiers in Microbiology*, vol. 13, article 849482, 2022.

[17] Y. Han, Y. Huang, P. Gao et al., "Leptin aggravates periodontitis by promoting M1 polarization via NLRP3," *Journal of Dental Research*, vol. 101, no. 6, pp. 675–685, 2022.

[18] M. Goto, "8. Image processing using ImageJ," *Nihon Hoshasen Gijutsu Gakkai Zasshi*, vol. 75, no. 7, pp. 688–692, 2019.

[19] K. Kure, H. Sato, J. I. Suzuki, A. Itai, N. Aoyama, and Y. Izumi, "A novel IkB kinase inhibitor attenuates ligature-induced periodontal disease in mice," *Journal of Periodontal Research*, vol. 54, no. 2, pp. 164–173, 2019.

[20] X. Hu, X. Jia, C. Xu et al., "Downregulation of NK cell activities in apolipoprotein C-III-induced hyperlipidemia resulting from lipid-induced metabolic reprogramming and crosstalk with lipid-laden dendritic cells," *Metabolism*, vol. 120, article 154800, 2021.

[21] J. E. Vince, D. Pantaki, R. Feltham et al., "TRAF2 must bind to cellular inhibitors of apoptosis for tumor necrosis factor (TNF) to efficiently activate NF-κB and to prevent TNF-induced apoptosis," *The Journal of Biological Chemistry*, vol. 284, no. 51, pp. 35906–35915, 2009.

[22] L. Yu, C. Zhou, Z. Wei, and Z. Shi, "Effect of combined periodontal-orthodontic treatment on NOD-like receptor protein 3 and high mobility group box-1 expressions in patients with periodontitis and its clinical significance," *Medicine (Baltimore)*, vol. 98, no. 44, article e17724, 2019.

[23] H. Wen, E. A. Miao, and J. P. Ting, "Mechanisms of NOD-like receptor-associated inflammasome activation," *Immunity*, vol. 39, no. 3, pp. 432–441, 2013.

[24] H. M. Jang, J. Y. Park, Y. J. Lee et al., "TLR2 and the NLRP3 inflammasome mediate IL-1β production in Prevotella nigrescens-infected dendritic cells," *International Journal of Medical Sciences*, vol. 18, no. 2, pp. 432–440, 2021.

[25] Y. Kawahara, T. Kaneko, Y. Yoshinaga et al., "Effects of sulfonylureas on periodontopathic bacteria-induced inflammation," *Journal of Dental Research*, vol. 99, no. 7, pp. 830–838, 2020.

[26] K. Shibata, "Historical aspects of studies on roles of the inflammasome in the pathogenesis of periodontal diseases," *Molecular Oral Microbiology*, vol. 33, no. 3, pp. 203–211, 2018.

[27] Y. Yamaguchi, T. Kurita-Ochiai, R. Kobayashi, T. Suzuki, and T. Ando, "Regulation of the NLRP3 inflammasome in Porphyromonas gingivalis-accelerated periodontal disease," *Inflammation Research*, vol. 66, no. 1, pp. 59–65, 2017.

[28] A. J. van Winkelhoff, P. Rurenga, G. J. Wekema-Mulder, Z. M. Singadji, and T. E. Rams, "Non-oral gram-negative facultative rods in chronic periodontitis microbiota," *Microbial Pathogenesis*, vol. 94, pp. 117–122, 2016.

[29] J. Ebersole, S. Kirakodu, J. Chen, R. Nagarajan, and O. A. Gonzalez, "Oral microbiome and gingival transcriptome profiles of ligature-induced periodontitis," *Journal of Dental Research*, vol. 99, no. 6, pp. 746–757, 2020.

[30] R. G. Fischer, S. Edwardsson, and B. Klinge, "Oral microflora of the ferret at the gingival sulcus and mucosa membrane in relation to ligature-induced periodontitis," *Oral Microbiology and Immunology*, vol. 9, no. 1, pp. 40–49, 1994.

[31] T. Kawai, B. J. Paster, H. Komatsuzawa et al., "Cross-reactive adaptive immune response to oral commensal bacteria results in an induction of receptor activator of nuclear factor-κB ligand (RANKL)-dependent periodontal bone resorption in a mouse model," *Oral Microbiology and Immunology*, vol. 22, no. 3, pp. 208–215, 2007.

[32] M. Radice, P. A. Martino, and A. M. Reiter, "Evaluation of subgingival bacteria in the dog and susceptibility to commonly used antibiotics," *Journal of Veterinary Dentistry*, vol. 23, no. 4, pp. 219–224, 2006.

[33] P. Pignatelli, G. Fabietti, A. Ricci, A. Piattelli, and M. C. Curia, "How periodontal disease and presence of nitric oxide reducing oral bacteria can affect blood pressure," *International Journal of Molecular Sciences*, vol. 21, no. 20, p. 7538, 2020.

[34] M. Harper, J. D. Boyce, and B. Adler, "Pasteurella multocida pathogenesis: 125 years after Pasteur," *FEMS Microbiology Letters*, vol. 265, no. 1, pp. 1–10, 2006.

[35] K. F. Kubatzky, B. Kloos, and D. Hildebrand, "Signaling cascades of Pasteurella multocida toxin in immune evasion," *Toxins (Basel)*, vol. 5, no. 9, pp. 1664–1681, 2013.

[36] E. Latz, T. S. Xiao, and A. Stutz, "Activation and regulation of the inflammasomes," *Nature Reviews. Immunology*, vol. 13, no. 6, pp. 397–411, 2013.

[37] J. H. Orth, I. Preuss, I. Fester, A. Schlosser, B. A. Wilson, and K. Aktories, "Pasteurella multocida toxin activation of heterotrimeric G proteins by deamidation," *Proceedings of the National Academy of Sciences of the United States of America*, vol. 106, no. 17, pp. 7179–7184, 2009.

[38] D. Hildebrand, K. A. Bode, D. Riess et al., "Granzyme A produces bioactive IL-1β through a nonapoptotic inflammasome-independent pathway," *Cell Reports*, vol. 9, no. 3, pp. 910–917, 2014.

[39] S. Chakraborty, B. Kloos, U. Harre, G. Schett, and K. F. Kubatzky, "<i>Pasteurella multocida</i> toxin triggers RANKL-independent osteoclastogenesis," *Frontiers in Immunology*, vol. 8, p. 185, 2017.

[40] J. K. Ebner, G. M. Konig, E. Kostenis, P. Siegert, K. Aktories, and J. H. C. Orth, "Activation of G_q signaling by _Pasteurella multocida_ toxin inhibits the osteoblastogenic-like actions of Activin A in C2C12 myoblasts, a cell model of fibrodysplasia ossificans progressiva," *Bone*, vol. 127, pp. 592–601, 2019.

[41] D. K. Khajuria, O. N. Patil, D. Karasik, and R. Razdan, "Development and evaluation of novel biodegradable chitosan based metformin intrapocket dental film for the management of periodontitis and alveolar bone loss in a rat model," *Archives of Oral Biology*, vol. 85, pp. 120–129, 2018.

[42] J. H. Kim, H. M. Jin, K. Kim et al., "The mechanism of osteoclast differentiation induced by IL-1," *Journal of Immunology*, vol. 183, no. 3, pp. 1862–1870, 2009.

[43] K. Aral, M. R. Milward, and P. R. Cooper, "Inflammasome dysregulation in human gingival fibroblasts in response to periodontal pathogens," *Oral Diseases*, vol. 28, no. 1, pp. 216–224, 2022.

[44] Z. Y. Qin, X. Gu, Y. L. Chen et al., "Toll-like receptor 4 activates the NLRP3 inflammasome pathway and periodontal inflammaging by inhibiting Bmi-1 expression," *International Journal of Molecular Medicine*, vol. 47, no. 1, pp. 137–150, 2021.

[45] R. C. Coll, J. R. Hill, C. J. Day et al., "MCC950 directly targets the NLRP3 ATP-hydrolysis motif for inflammasome inhibition," *Nature Chemical Biology*, vol. 15, no. 6, pp. 556–559, 2019.

[46] A. Tapia-Abellan, D. Angosto-Bazarra, H. Martinez-Banaclocha et al., "MCC950 closes the active conformation of NLRP3 to an inactive state," *Nature Chemical Biology*, vol. 15, no. 6, pp. 560–564, 2019.

[47] R. C. Coll, A. A. Robertson, J. J. Chae et al., "A small-molecule inhibitor of the NLRP3 inflammasome for the treatment of inflammatory diseases," *Nature Medicine*, vol. 21, no. 3, pp. 248–255, 2015.

[48] Y. Han, P. Gao, Q. Yang et al., *Pasteurella multocidia toxin aggravates ligatured-induced periodontal bone loss and inflammation via NOD-like receptor protein 3 inflammasome*, Research Square, 2022.